Journal of Controlled Release 305 (2019) 210–219

Contents lists available at ScienceDirect

Journal of Controlled Release

journal homepage: www.elsevier.com/locate/jconrel

Cationic block amphiphiles show anti-mitochondrial activity in multi-drug resistant breast cancer cells

Petro P. Czupiel[a,b,c], Vianney Delplace[a,c], Molly S. Shoichet[a,b,c,*]

[a] Department of Chemical Engineering and Applied Chemistry, University of Toronto, 200 College Street, Toronto, ON M5S 3E5, Canada
[b] Institute of Biomaterials and Biomedical Engineering, University of Toronto, 164 College Street, Toronto, ON M5S 3G9, Canada
[c] Donnelly Centre, University of Toronto, 160 College Street, Toronto, ON M5S 3E1, Canada

ARTICLE INFO

Keywords:
Peptides
Mitochondrial targeting
Cancer
Multi-drug resistance
Vitamin E
Prodrug

ABSTRACT

Currently, there are limited treatment options for multi-drug resistant breast cancer. Lipid-modified cationic peptides have the potential to reach the mitochondria, which are attractive targets for the treatment of multi-drug resistant (MDR) breast cancer; yet, little is known about their mitochondrial targeting and anti-cancer activity. Interestingly, lipid-modified cationic peptides, typically used as gene transfection agents, exhibit similar structural features to mitochondrial targeted peptides. Using octahistidine-octaarginine (H_8R_8) as a model cationic peptide for cell penetration and endosomal escape, we explored the anti-cancer potential of lipid-modified cationic peptides as a function of amphiphilicity, biodegradability and lipid structure. We found that cationic peptides modified with a lipid that is at least 12 carbons in length exhibit potent anti-cancer activity in the low micromolar range in both EMT6/P and EMT6/AR-1 breast cancer cells. Comparing degradable and non-degradable linkers, as well as L- and D-amino acid sequences, we found that the anti-cancer activity is mostly independent of the biodegradation of the lipid-modified cationic peptides. Two candidates, stearyl-H_8R_8 (Str-H_8R_8) and vitamin E succinate-H_8R_8 (VES-H_8R_8) were cytotoxic to cancer cells by mitochondria depolarization. We observed increased reactive oxygen species (ROS) production, reduced cell bioenergetics and drug efflux, triggering apoptosis and G1 cell cycle arrest. Compared to Str-H_8R_8, VES-H_8R_8 showed enhanced cancer cell selectivity and drug efflux inhibition, thereby serving as a potential novel therapeutic agent. This study deepens our understanding of lipid-modified cationic peptides and uncovers their potential in multi-drug resistant breast cancer.

1. Introduction

Mitochondria are the powerhouse of the cell and serve as an attractive target for cancer treatment. In cellular processes, these organelles provide adenosine triphosphate (ATP) through oxidative phosphorylation, constitute the main source of reactive oxygen species (ROS), and participate in oxidative signaling, thereby playing a critical role in the rapid proliferation of cancer cells [1–3]. Oncogenic activation leads to increased mitochondrial metabolism and higher mitochondrial membrane potential compared to that of non-cancer cells [1,4]. Moreover, multi-drug resistant (MDR) cancer cells exhibit increased mitochondrial mass with more polarized mitochondria relative to non-MDR cells [5]. As MDR arises from the overexpression of drug efflux pumps, which requires ATP from mitochondria, mitochondrial targeting is a particularly sensible option for the treatment of drug-resistant cancer cells [1,6,7]. Hence, the more polarized mitochondria membranes in cancer cells together with the ATP-dependent drug efflux introduces an important target in MDR cancer cells.

Targeting mitochondria requires penetration through cellular and mitochondrial membranes [8]. Cationic amphiphilic structures are excellent candidates for mitochondrial targeting as they can interact with negatively charged cellular and mitochondrial membranes [8,9,10]. Mitochondrial-penetrating peptides (MPPs) have been designed with alternating amino acids containing delocalized lipophilic cationic side groups, such as arginine, and hydrophobic amino acids, such as cyclohexylalanine [8]. Primarily used at low concentrations for mitochondria imaging, these peptides have been shown to potentiate the activity of chemotherapeutics or reduce the side effects of antimicrobials [8,11]. At a threshold concentration, they inhibit oxidative phosphorylation and electron transport chain, collapse mitochondria and induce apoptosis [8]. Similarly, cationic amphiphilic polymers, such as poly(ethylenimine) (PEI), form pores in mitochondria

* Corresponding author at: Department of Chemical Engineering and Applied Chemistry, University of Toronto, 200 College Street, Toronto, ON M5S 3E5, Canada.
E-mail address: molly.shoichet@utoronto.ca (M.S. Shoichet).

https://doi.org/10.1016/j.jconrel.2019.04.045
Received 23 November 2018; Received in revised form 17 April 2019; Accepted 29 April 2019
Available online 06 May 2019
0168-3659/

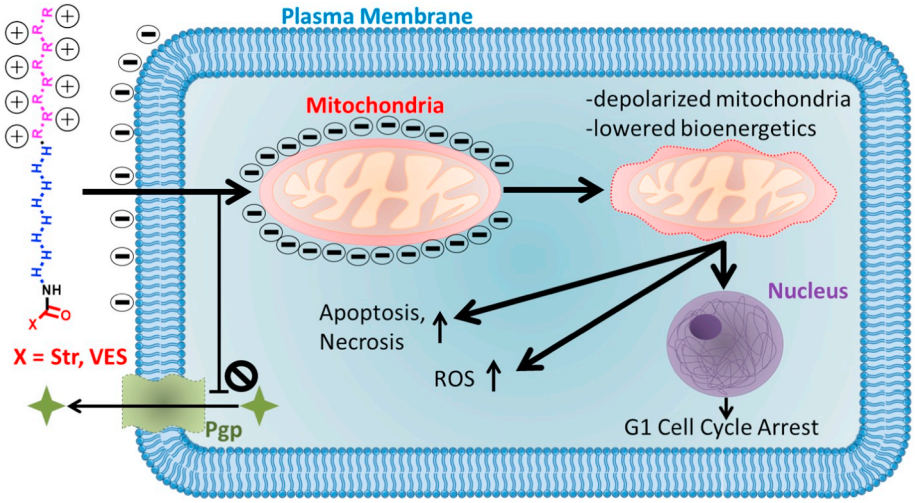

Fig. 1. Schematic of the mechanism of cancer cell death following treatment with vitamin E succinate modified octaarginine-octahistidine (VES-H_8R_8). VES-H_8R_8 is taken up through electrostatic interaction with the plasma membrane and depolarizes the mitochondria through a mitochondrial permeability transition pore (mPTP)-dependent pathway (dotted red line). Consequently, bioenergetics of the mitochondria are inhibited, ROS are elevated, both apoptosis and necrosis are induced, and cells are arrested at the G1 phase. VES-H_8R_8 was shown to decrease the efflux capability of permeation glycoprotein (Pgp). VES represents vitamin E succinate moiety and Str represents a stearyl moiety. (For interpretation of the references to colour in this figure legend, the reader is referred to the web version of this article.)

membranes, causing proton leakage and depolarization, and thereby induce apoptosis [12]. Interestingly, lipid-modified cationic peptides, composed of a cationic cell penetrating peptide and a fatty acid chain, closely resemble MPPs in structural properties; yet, their anti-mitochondrial activity remain understudied and poorly understood. This knowledge gap prompted us to investigate the activity of lipid-modified cationic peptides as mitochondria-targeting drugs for cancer treatment. We hypothesized that such lipid-modified cationic peptides could selectively target and depolarize the mitochondria of MDR breast cancer cells (Fig. 1).

Using the octahistidine-octaarginine (H_8R_8) peptide as a common cationic cell penetrating peptide with endosomal escape capabilities, we investigated, for the first time, the intracellular fate and effects of lipid-modified cationic peptides in breast cancer cells [13,14]. First, we studied the anticancer activity of H_8R_8-based amphiphiles in relation to hydrophobicity and degradability. Comparing a biologically inert hydrophobic stearyl chain-modified H_8R_8 to the bioactive MDR sensitizer, vitamin E succinate (VES)-modified peptide, we investigated cancer cell toxicity and cancer selectivity relative to healthy cells [15,16]. We explored the intracellular effects of H_8R_8-based cationic lipids and evaluated mitochondrial inhibition, induction of ROS accumulation, apoptosis, necrosis, and cell cycle arrest. VES-H_8R_8 was also investigated for inhibition of permeation glycoprotein (Pgp) efflux in MDR breast cancer cells. Herein, we highlight H_8R_8-based amphiphiles, and specifically vitamin E-based prodrugs for MDR breast cancer cell targeting.

2. Materials and methods

All solvents and reagents were purchased from Sigma-Aldrich and used as received unless otherwise noted. Peptide synthesis reagents were purchased from AnaSpec (Fremont, CA).

2.1. Peptide synthesis

H_8R_8 was synthesized by conventional solid-phase microwave assisted peptide synthesis techniques (CEM Liberty 1) where double histidine and arginine couplings were employed. To make amide peptides, rink amide ProTide Resins were used (CEM Corp, NC, USA). Standard microwave-assisted Fmoc deprotection was used [17]. Peptides were prepared at 0.25 mmol scale using HOBt/DIC/Oxyma for activation. Fmoc-Arg(Pbf)-OH was purchased from Ark Pharm (Illinois, USA) and Fmoc-His(Trt)-OH were from EMD Millipore (Massachusetts, USA).

2.2. Synthesis of vitamin E-oxy-butyric acid

Vitamin E was modified as follows: in a 250-mL round-bottom flask, 417.69 mg (1.46 eq) of NaH were dissolved in 50 mL of THF and stirred on ice under argon for 10 min. 5.12 g (1 eq) of Vitamin E (α-tocopherol) were dissolved in 50 mL of THF and added to the NaH solution, before stirring on ice for 15 min under argon. 2.492 mL (1.46 eq) of bromoethyl butyrate were added to the solution before stirring under argon first on ice for 20 min and then at room temperature overnight. The solution was transferred to a large beaker and diluted with 300 mL of CH_2Cl_2. Liquid-liquid extraction with excess DI water was used to purify the Vitamin *E*-oxy-ethylbutyrate intermediate (ESI-MS^+: $C_{35}H_{60}O_4$ expected *m/z* 544.9, found m/z 545.5 corresponding to M + H). 1 g of Vitamin E-oxy-ethylbutyrate was hydrolyzed in a mix of 10% *w/v* KOH (5 mL) and THF (10 mL) overnight. The solution was then quenched with 10 mL DI water, adjusted to pH 3 with concentrated HCl (5–10 drops), and extracted 3 times with CH_2Cl_2. The organic phase was washed 2 times with saturated NaCl solution, dried on MgSO4 and evaporated under vacuum to give the final product. The crude was then purified on a silica column, using chloroform as eluting solvent. Impurities were washed off in chloroform, and the final product was eluted in chloroform:methanol (9:1 *v/v*). The organic solvent was removed by rotary evaporation and dried in an oven. (ESI-MS: $C_{33}H_{56}O_4$ expected *m/z* 516.8, found 515.4 corresponding to M-H).

2.3. N-terminal peptide acylation

To modify the N-terminus of the peptide (0.125 mmol), 4.9 eq. of HCTU were used to activate 5.0 eq. of acid (stearic acid or vitamin e succinate) in DMF for 15 min at room temperature. The activated acid was then added to the peptides on resin, while adding 1 eq. of N,N-diisopropylethylamine (DIPEA). The reaction was allowed to proceed for 24 h before the resin was washed 2 times with DMF, then 2 times with DCM. Conjugation was evaluated with the 2,4,6-Trinitrobenzenesulfonic acid (TNBS) test [18].

2.4. Fluorescein labeling of peptide

To synthesize the fluorescein-modified peptide, Fmoc-Lys(alloc)-OH (EMD Millipore, Massachusetts, USA) was used and inserted between H_8 and R_8 as NH_2-H_8K(Alloc)-R_8-Resin. VES and stearic acid were separately conjugated to the N-terminus using HCTU as above. Then the alloc protecting group was deprotected 3-times, 20 min each, using 0.1 eq. of tetrakis(triphenylphosphine) palladium(0) (Pd(PPh3)), and 10 eq. of borane dimethylamine complex ($Me_2NH{\cdot}BH_3$). Finally, 5(6)-Carboxyfluorescein was activated using HCTU and conjugated to the

peptide as stated above. Fmoc-NH_2-H_8K(Alloc)-R_8-Resin was used to prepare the fluorescein modified H_8R_8 where alloc was deprotected as above, and fluorescein was added to the free amine on lysine as above. Fmoc was then deprotected using 20% piperidine in DMF.

2.5. Cleavage and purification

Final deprotection and cleavage off of the resin was completed using a cleavage cocktail composed of trifluoroacetic acid:water:-triisopropylsilane (TFA:H_2O:TIS, 95:2.5:2.5 v/v/v) for 5 h. The peptide was then precipitated in cold ether, centrifuged and washed with cold ether and allowed to dry overnight. The precipitate was then dissolved in TFA, diluted in acetonitrile:water (ACN:H_2O:TFA, 90:9.9:0.1 v/v/v), and purified through a C18 reverse phase column (Silicycle, Quebec, Canada) using a gradient of acetonitrile from 10 to 100%. Peptide mass was verified through electrospray ionization (EI) or matrix assisted laser desorption ionization-time of flight (MALDI-TOF) mass spectrometry using the Agilent 6538 Q-TOF mass spectrometer. Stock solutions of peptides were prepared in DMSO.

2.6. Nanoparticle characterization and critical micelle concentration measurements

Str-H_8R_8 and VES-H_8R_8 were dissolved in DMSO at a concentration of 250 mg/mL, and diluted in PBS (pH 7.4), 1.5 μM citric acid in PBS (pH 6.3), or 3 μM citric acid in PBS (pH 5.3). The peptides were passed through a 0.2 μm polyethylsulfone (PES) filter and nanoparticle diameters were measured using a Malvern Zetasizer Nano ZS (4 mW, 633 nm laser) at a concentration of 2.5 mg/mL. Critical micelle concentration (CMC) was calculated based on the scattering intensity measured by dynamic light scattering as previously described [19]. The scattering intensity was measured using a DynaPro Plate Reader II (Wyatt Technologies) configured with a 60 mW, 830 nm laser and a detector angle of 158°. Str-H_8R_8 and VES-H_8R_8 were added to clear bottom 96-well plates at a peptide concentration of 16.6 mg/mL in PBS (pH 7.4), and serially diluted with measurements of three acquisitions per sample. Curve fitting algorithms were used to determine the CMC of the nanoparticles.

2.7. Cell culture

Both parental (EMT6/P) and doxorubicin resistant (EMT6/AR1) EMT6 cells were generously provided by Dr. X.Y. Wu (University of Toronto), originally from Dr. Ian F. Tannock at the Ontario Cancer Institute, (Toronto, ON, Canada) and maintained in our laboratory. Non-cancerous fibroblast cells (NIH/3T3) were grown in DMEM media supplemented with 10% fetal calf serum and 1% penicillin/streptomycin and grown as above. EMT6/P cells were grown in α-MEM medium supplemented with 10% FBS, 1% penicillin/streptomycin at 37 °C in a humidified incubator with 5% CO_2 atmosphere. EMT6/AR-1 cells were grown as above, with the addition of doxorubicin at 1 μg/mL to maintain doxorubicin resistance and permeation glycoprotein (Pgp) overexpression.

2.8. Cell culture cytotoxicity assay

Cells were seeded into 96-well flat-bottomed tissue culture plates at a density of 3000 cells per well and allowed to adhere for 24 h. H_8R_8 peptides dissolved in DMSO were serially diluted in PBS and then into full medium, and incubated with cells for 72 h. The doses chosen were based on the observed inhibitor concentration to kill 50% of the cells (IC_{50}). Similar DMSO concentration was used as a control. DMSO was used at concentration $< 0.5\%$ *v*/v. After the addition of peptides, cells were allowed to grow for 72 h at 37 °C in a 5% CO_2 and 95% air humidified incubator. Presto Blue (Life Technology) was added to fresh medium as per the manufacturer's protocol and incubated with cells for 1.5 h. Viable cells are able to reduce the resazurin dye in Presto Blue to a highly red fluorescent resorufin (ex/em 540/590 nm) which can be read by a microplate fluorescent reader (Infinit m200 Pro, Tecan Group Ltd., Switzerland). Each measurement is an average of 3 separate passages of cells. Dose response curves and inhibitor concentration to kill 50% of the cells (IC_{50}) were obtained from Graph Pad Prism version 6.00 for Windows (Graph Pad Software, CA, USA, www.graphpad.com). Relative viability was calculated as the fluoresce intensity of the treated group divided by the fluorescence intensity of a control group.

2.9. Laser scanning confocal microscopy

EMT6/P cells were seeded at a density of 20,000 cells per well in a 8-well Nunc Lab-Tek II chambered cover glass (Thermo Fisher Scientific, MA, USA) and allowed to adhere for 24 h at 37 °C in a 5% CO_2 and 95% air humidified incubator. 0.8 μM of fluorescein-modified peptide was added to the cells and incubated for 3 h. The peptide containing media was aspirated off, and 200 nM of MitoTracker Deep Red FM (Thermo Fisher, MA, USA) in full media was added to the cells. After 15 min incubation, the cells were washed 3-times with PBS, and then Hoescht 33,342 nuclei acid dye (Molecular Probes, Inc., Eugene, OR, USA) in PBS was added to the cells. Live cell imaging was done using an Olympus FV1000 confocal microscope equipped with an oil immersion 60× lens. Excitation and emission wavelengths are as follows: Hoescht 33,342 (ex/em: 405/460 nm) fluorescein (ex/em 488/520 nm), MitoTracker Deep Red FM, (ex/em: 640/670 nm). Unlabeled control cells were used to set the laser power to avoid fluorescent bleed over between channels.

2.10. Fluorescein-modified peptide uptake in intact cells and isolated mitochondria

The uptake of the VES-H_8R_8, Str-H_8R_8 in the mitochondria of intact cells was quantified as previously reported [20]. 5×10^6 cells were seeded in T-25 flasks and allowed to adhere for 24 h at 37 °C in a 5% CO_2 and 95% air humidified incubator. Non-toxic concentrations of peptides were used (< 0.8 μM). The EMT6/AR-1 cells were treated the next day with the fluorescein-modified peptides of VES-H_8R_8, Str-H_8R_8, or H_8R_8 (0.8 μM), or free fluorescein as a dye control (0.8 μM). The cells were incubated with peptides or dye control for 3 h in full medium, and then the cells were harvested with trypsin. After centrifugation, mitochondria from the pelleted cells were extracted according to the instructions of the Mitochondria Isolation Kit for cultured cells (Thermo Fisher Scientific, MA, USA). cOmplete Mini, EDTA free protease inhibitor cocktail was added to reagents A and C of the mitochondrial isolation kit with 1 tablet/10 mL of extraction buffer. A more purified fraction of mitochondria was obtained by centrifuging the post-nuclear supernatant at 3000 ×*g*. The mitochondria pellet was then suspended in PBS, transferred into a 96-well clear bottom black plate and fluorescein was quantified (ex/em 490/520 nm) against a standard curve in PBS using a Tecan Plate Reader. The average of three biological repeats was used to measure the amount of fluorescein uptake.

The uptake of the fluorescein-modified peptides of VES-H_8R_8, Str-H_8R_8, H_8R_8, or free fluorescein was also investigated with isolated mitochondria as reported previously [20]. Mitochondria from 1.1×10^8 cells of untreated EMT6/AR-cells were extracted according to the previous section. The mitochondria of approximately 6×10^6 cells were then suspended in mitochondria isolation buffer (10 mM Tris hydrochloride, 0.15 mM $MgCl_2$, 0.25 mM sucrose, 1 mM DTT, pH 6.7, and 1 tablet/10 mL of cOmplete, Mini, EDTA free protease inhibitor cocktail) and fluorescein-modified peptides of VES-H_8R_8, Str-H_8R_8, H_8R_8, or free fluorescein were added at a final concentration of 0.8 μM. The isolated mitochondria were incubated with the peptides or free fluorescein for 1 h at 37 °C, and then washed with PBS three times by centrifuging at 12,000 ×*g* for 5 min. The isolated mitochondria were then suspended in PBS, transferred into a 96-well clear bottom black

plate and fluorescein was quantified (ex/em 490/520 nm) against a standard curve in PBS using a Tecan Plate Reader. The average of three biological repeats was used to measure the amount of fluorescein uptake.

2.11. Fluorescein-modified peptide uptake and retention studies

20,000 cells were seeded into 48-well plates and allowed to adhere for 24 h at 37 °C in a 5% CO_2 and 95% air humidified incubator. Non-toxic concentrations of peptides were used (< 0.8 μM). The EMT6/AR-1 cells were treated with the fluorescein-modified peptides (0.8 μM) for 2, 5, or 24 h in full media. The fluorescein retention study was completed by incubating with either peptides alone or co-incubation of Str-H_8R_8 (0.8 μM) with free VES (20 μM) for 24 h, followed by 24 h in fresh media. A similar DMSO concentration was used as a control. After treatment, cells were washed 3 times with PBS, and harvested with trypsin. Cell fluorescence was analyzed using a BD Accuri C6 flow cytometer with excitation wavelength of 488 nm and emission filters of 533/30 nm (fluorescein, FL-2 channel). Cell debris and doublets were gated out using FSC-A vs FSC-H, and at least 10,000 events were collected. The mean fluorescence intensity in the FL-1 channel (ex/em 488/533(30) nm) for three biological repeats was used to measure the amount of fluorescein uptake.

2.12. Mitochondrial membrane polarization assay

Mitochondrial membrane potential was assayed using the JC-1 probe (5,5′,6,6′-tetrachloro-1,1′,3,3′-tetraethylbenzimidazolylcarbocyanine iodide) (ex/em 488 nm/533–585 nm) (Biotium Inc., CA, USA) [21]. 20,000 cells were seeded into 48-well plates and allowed to adhere for 24 h at 37 °C in a 5% CO_2 and 95% air humidified incubator. The cells were treated the next day for 2 or 5 h in full media. Control treatments and peptides were incubated at 8 μM, in the range of the IC_{50} of both Str-H_8R_8 and VES-H_8R_8. A similar DMSO concentration was used as a control. Carbonyl cyanide *m*-chlorophenyl hydrazone (CCCP) at 50 μM was used as a positive control for mitochondrial depolarization. Following treatment, the cells were washed with PBS 3 times and then incubated at 37 °C with 10 μM of JC-1 in full media for 30 min. The EMT6/P cells were incubated with 2 μM of JC-1 in full media to avoid fluorescent saturation in the flow cytometer. The cells were then washed 3 times in PBS, trypsinized, and placed on ice before measuring fluorescence in a flow cytometer within 1 h. Cell debris and doublets were gated out using FSC-A vs FSC-H, and at least 10,000 events were collected. A gate was set according to DMSO and CCCP treated cells in the FL-2 channel (ex/em 488 nm/585(40) nm) to measure the proportion of JC-1 aggregate fluorescence versus JC-1 monomer fluorescence in the FL-1 channel (ex/em 488 nm/533(30) nm). To assess the mitochondrial permeability transition pore formation, cyclosporine A was used as previously described [21]. Averages were obtained from three biological repeats. Changes in the mitochondria membrane potential (ΔΨm) were expressed using the following equation:

$$\textit{Relative Mitochondrial Membrane Potential } (\Delta\Psi m) = \frac{\frac{JC1_{aggregate}}{JC1_{monomer\ Treatment}}}{\frac{JC1_{aggregate}}{JC1_{monomer\ Control}}}\ x\ 100\%$$

2.13. Real-time investigation of Oxygen Consumption Rate (OCR) and Extracellular Adcification rate (ECAR)

Analyses of bioenergetics processes were performed in intact EMT6/P and EMT6/Ar-1 cells using the Seahorse XF Analyzer (Agilent, CA, USA). An optimized cell density of 10,000 cells/well were seeded in a XF96 V4 cell culture microplate and allowed to adhere for 24 h at 37 °C in a 5% CO_2 and 95% air humidified incubator. Oxygen consumption rate (OCR) and extracellular acidification rate (ECAR) were measured as cells were incubated with 30 μM of VES-H_8R_8 or Str-H_8R_8 for 2 h before inhibitors were added. An optimized concentration of 1 μM of carbonyl cyanide *p*-triflouromethoxyphenylhydrazone (FCCP) was used. Basal respiration, proton leak, ATP production and maximum-respiratory rate were calculated as reported before and averaged from three biological repeats [22].

2.14. ROS production assay

Reactive oxygen species (ROS) in cells were detected using 5-(and-6)-carboxy-2,7-dichlorodihydrofluorescein diacetate (CDCFDA) (AAT Bioquest, CA, USA) as previously described [23]. 20,000 cells were seeded into 48-well plates and allowed to adhere for 24 h at 37 °C in a 5% CO_2 and 95% air humidified incubator. The cells were treated the next day for either 2 or 5 h in full media. Control treatments and peptides were incubated at 8 μM, in the range of the IC_{50} of both Str-H_8R_8 and VES- H_8R_8. A similar DMSO concentration was used as a control. Hydrogen peroxide (H_2O_2) at 1 mM was used as a positive control. Following treatment, cells were washed with PBS 3 times, and then incubated at 37 °C in full media containing 2 μM CDCFDA for 30 min. The cells were washed 3 times with PBS, harvested, and placed on ice before measuring fluorescence using a flow cytometer within 1 h. Cell debris and doublets were gated out using FSC-A vs FSC-H, and 10,000 events were collected. The mean fluorescence intensity was collected in the FL-1 channel (ex/em 488/533(30) nm) and averaged from three biological replicates. The results were expressed as fold increase in mean fluorescence intensity of treated group relative to DMSO control. To assess the radical scavenger capability of free vitamin E, 100 μM of vitamin E was incubated simultaneously with peptide treatments (8 μM) for 5 h and ROS was measured as stated above.

2.15. Apoptosis induction assay

Apoptosis was measured using Annexin V-Cy5 (Biovision Inc., CA, USA) and 7-aminoactinomycin D (7-AAD) (AAT Bioquest, CA USA) [24,25]. 20,000 cells were seeded into 48-well plates and allowed to adhere for 24 h at 37 °C in a 5% CO_2 and 95% air humidified incubator. The cells were treated the next day with peptides at 5, 10, and 20 μM for 2 h in full media. A similar DMSO concentration was used as a control. Following treatment, floating cells were collected, adhered cells were harvested, washed with PBS, and then incubated with Annexin V-Cy5 (1 μL/mL) and 7-AAD (15 μg/mL) for 20 min at 25 °C as per the manufacturer's protocol. Cells were then placed on ice before measuring fluorescence in a flow cytometer within an hour. Cell debris and doublets were gated out using FSC-A vs FSC-H, and at least 10,000 events were collected. Using the untreated control group, gates were set in the FL-3 (ex/em 488/ > 670 nm) and FL-4 channel (ex/em 640/675(25) nm) for 7-AAD and Annexin-V-Cy5 respectively, and identical gates were used for the other treatment groups. Proportion of apoptotic or necrotic cells were averaged from 3 biological repeats.

2.16. Cell cycle analysis

Cell cycle analysis was performed using 7-AAD (7-aminoactinomycin D) (AAT Bioquest, CA USA). 20,000 cells were seeded into 48-well plates and allowed to adhere for 24 h at 37 °C in a 5% CO_2 and 95% air humidified incubator. The cells were treated the next day for 24 h in full media. Control treatments and peptides were incubated at 15 μM. A similar DMSO concentration was used as a negative control. Following treatment, the cells were harvested, washed with PBS, then incubated with 25 μg/mL of 7-AAD in PBS containing 1% bovine serum albumin (BSA) and 0.15% Triton X for 25 min. Cells were placed on ice before measuring fluorescence in a flow cytometer. Cell debris and doublets were gated out using the FSC-A vs FSC-H, and 10,000 events were collected. The FL-3 channel (ex/em 640/ > 670 nm) was set in a linear range, and cell cycle analysis was completed using the FlowJo software

(Flowjo, OR, USA) using the Watson Pragmatic Mod Fit algorithms. The results were expressed as proportion of cells in the G1, S, and G2 phases relative to DMSO control, and averaged from three biological repeats.

2.17. Statistical analysis

All statistical analyses were performed using Graph Pad Prism version 6.00 for Windows (Graph Pad Software, San Diego, California, www.graphpad.com). Differences among groups were assessed by one-way ANOVA with Tukey's multiple comparison test. Alpha levels were set at 0.05 and a p-value of < 0.05 was set as the criteria for statistical significance. Graphs are annotated with p-values as $^{*}p < .05$, $^{**}p < .01$, or $^{***}p < .001$. All data are presented as mean ± standard deviation.

3. Results and discussion

3.1. H_8R_8-based cationic lipids have selective anti-cancer activity

To investigate the effect of the lipid modification of H_8R_8 on its anti-cancer properties, the half maximum inhibitory concentration (IC_{50}) was evaluated with two breast cancer cells, parental breast cancer cells, EMT6/P, and the permeation glycoprotein (Pgp) overexpressing, MDR variant, EMT6/AR-1. We used the resazurin-based Presto Blue metabolic assay as a proxy to evaluate cell survival. Both Str-H_8R_8 and VES-H_8R_8 exhibited an IC_{50} in the low micromolar range while the unmodified peptide control, H_8R_8, exhibited an IC_{50} above 300 μM in both cancer cell lines (Fig. 2A, Supplementary Table S1). Similarly to unmodified H_8R_8, poly(ethylene glycol) (PEG)-modified H_8R_8 showed no cytotoxicity, confirming the necessity of providing a lipophilic character to H_8R_8 cationic peptides for anti-cancer activity (Fig. S3A). While not attributed to the cationic amphiphilic structure by the authors, a similar strategy was employed with the cationic Tat peptide, which, when conjugated to paclitaxel, resulted in enhanced anti-cancer activity with increased paclitaxel uptake in MDR cancer cells relative to paclitaxel alone [26]. Here, the unmodified Tat peptide was non-toxic to the cancer cells while the Tat modified paclitaxel exhibited potent anti-cancer activity in both parental and MDR cancer cells. In our study, both Str-H_8R_8 and VES-H_8R_8 had similar activities on each cell line, with an IC_{50} on EMT6/P of 4.2 ± 0.1 μM and 4.4 ± 0.1 μM, respectively; and an IC_{50} on EMT6/AR-1 of 6.8 ± 0.3 μM and 7.3 ± 0.3 μM, respectively. While the pK_a of histidine is 6.0 and intratumoral pH can range between 6.5 and 6.9, we do not anticipate that the more acidic tumor environment would enhance the anti-cancer activity of both Str-H_8R_8 and VES-H_8R_8 as the histidine would remain deprotonated [27–29]. Interestingly, due to the amphiphilic nature of the modified peptides, Str-H_8R_8 and VES-H_8R_8 formed nanoparticles in PBS exhibiting diameters of 11.1 nm ± 0.3 nm and 10.9 nm ± 0.2 nm, respectively, and nanoparticle diameters did not change in acidic buffer with pH 5.3 (Fig. S1A, B and Table S2). Importantly, both Str-H_8R_8 and VES-H_8R_8 nanoparticles exhibited high critical micelle concentrations > 257 μM, indicating that both peptides exist as non-aggregated unimers in the low 0–20 μM range used (Fig. S1C,D and Table S2). For both lipid-modified cationic peptides, there was a significant increase in IC_{50} ($p < .001$) on MDR cancer cells compared to the parental cell line, suggesting that the activity of the H_8R_8-based amphiphiles was partially dependent on Pgp efflux activity. Pgp is able to efflux both hydrophobic and hydrophilic drugs, thereby reducing the effective intracellular drug concentration. For example, Pgp has been shown to efflux docetaxel and doxorubicin, requiring 100-fold more drug to kill MDR cancer cells than non-resistant cancer cells, whereas lipid-modified cationic peptides bypass the efflux capabilities [30,31]. Consistent with the literature, VES alone exhibited some anti-cancer activity, with IC_{50} values of 23.0 ± 2.0 μM and 36.0 ± 4.6 μM on EMT6/P and EMT6/AR-1, respectively [32,33]. Covalent modification of VES to H_8R_8 led to a 5-fold decrease in IC_{50} on both EMT6/P and EMT6/AR-1 relative to VES alone.

We compared the anti-cancer activity of protease resistant D-amino acid-based lipid-modified cationic peptides to that of their faster degrading L-amino acid counterparts [34]. Surprisingly, only a modest decrease in the IC_{50} was observed using the D-amino acid containing H_8R_8-based amphiphiles (Table S1). The enhanced activity may be attributed to the lower binding affinity to membrane-associated heparin sulfates and/or slower rates of internalization, as previously reported for similar cell penetrating peptides [35]. Thus, we used L-amino acid-based amphiphiles going forward as the L-amino acid peptides are naturally present in the body and the reduced degradability of D-amino acid containing peptides may be toxic to non-cancer cells [34].

To confirm the anticancer selectivity of H_8R_8-based amphiphiles, the IC_{50} of each amphiphile against MDR cancer cells was compared to that of non-cancer cells. NIH/3T3 cells were selected as the non-cancer cell line as fibroblasts are major stromal cells and they would typically be in close proximity to cancer cells [36]. Cancer selectivity is typically deduced from the difference in IC_{50} between cancer and endothelial or fibroblast cells [37]. The IC_{50} of VES-H_8R_8 and Str-H_8R_8 on healthy cells was up to 8.4-fold and 4.3-fold higher, respectively, than that of breast cancer cells ($p > .001$, Fig. 2A), demonstrating greater selective toxicity to cancer vs. healthy cells. Interestingly, the selectivity that we observed is consistent in order of magnitude with that observed of the clinical chemotherapeutic, docetaxel, where the IC_{50} on NIH/3 T3 cells is 6.4 fold higher than that on breast cancer EMT6/P cells (50 nM vs 7.8 nM) [38,39]. In both breast cancer cell lines investigated, VES-H_8R_8 was twice as selective compared to Str-H_8R_8, which may be due to the cancer selective activity reported for VES alone [37,40,41]. The anti-cancer selective activity of both VES-H_8R_8 and Str-H_8R_8 may arise from differences in cell membrane composition (e.g., o-glycosylated mucin concentration), mitochondrial polarization and greater cell proliferation of cancerous vs healthy cells [42–44]. The difference in membrane potential is attributed to healthy cells exposing more zwitterionic phospholipids vs cancer cells exposing more anionic phospholipids and negatively charged glycoproteins [44,45]. The mitochondrial membrane potential is typically more negative in cancerous than healthy cells. For example, Neu4145 cancer cells exhibit a mitochondria membrane potential of −210 mV whereas healthy cells typically exhibit a mitochondrial membrane potential in the range of −108 to

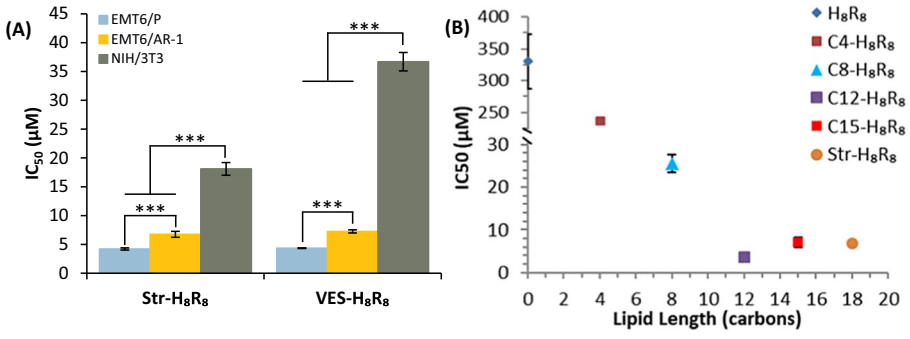

Fig. 2. H_8R_8-based amphiphiles exhibit potent and selective anti-cancer activity. (A) Comparison of the IC50 of Str-H_8R_8 and VES-H_8R_8 on the parental breast cancer cell line, EMT6/P, the multi-drug resistant breast cancer cell line, EMT6/AR-1, and the healthy fibroblast cell line, NIH/3T3. (B) Relationship between the anti-cancer activity on EMT6/AR-1 cells and the lipid length of the various H_8R_8-based amphiphiles. Data are presented as a mean ± SD ($n = 3$) and statistical analyses was performed using one-way ANOVA and Tukey's multiple comparison test (***p < .001).

−159 mV, which makes cancer cells more sensitive to mitochondria selective treatment [9,15]. As drug sensitive and MDR cancer cells exhibit more polarized mitochondria relative to non-cancerous cells, we anticipate that VES-H_8R_8 and Str-H_8R_8 will be potent against other drug sensitive and MDR cancer cells.

To gain greater insight into the role of the hydrophobic tail to anti-cancer activity, we measured the IC_{50} of a series of H_8R_8-based amphiphiles as a function of the lipid length of the amphiphilic peptides on EMT6/AR-1 (Fig. 2B) and EMT6/P cells (Fig. S3B). Both unmodified H_8R_8 and butyl-modified H_8R_8 showed limited anti-cancer activity, with IC_{50} above 200 μM. However, octyl-modified H_8R_8 exhibited an IC_{50} of 25.6 ± 1.9 μM, and longer hydrophobic segments (C_{12} and longer) exhibited IC_{50} in the low μM range (< 7 μM). These results suggest that H_8R_8-based amphiphiles modified with a lipid greater than or equal to 12 carbons is the threshold for anti-cancer activity. The enhanced anti-cancer activity of longer hydrophobic tails is likely due to enhanced membrane association and cell penetration, as was observed for C_{10}-C_{16} modified heptaarginine (R_7) [46]. Interestingly, mitochondrial-penetrating peptides with a logP in the range of −1.0 to −1.4 exhibited superior mitochondrial targeting relative to less hydrophobic peptides, highlighting a potential relationship between mitochondrial colocalization and anti-cancer activity [8]. We chose to further investigate Str-H_8R_8 and VES-H_8R_8 for cytotoxicity and targeting as the stearyl and VES moieties share similar theoretical logP values. While VES is known to be bioactive and Str-H_8R_8 has been used in gene delivery and nanoparticle formulations, there may be important and untapped synergistic effects encapsulating VES-H_8R_8 or Str-H_8R_8 [47,48]. Moreover, stearyl-modified cationic peptides have been used for nanoparticle-based drug delivery systems in vivo, where we anticipate that safe doses may be used with VES-H_8R_8 or Str-H_8R_8, prompting further in vivo investigations [49,50].

3.2. Bioactive VES-modified cationic peptides enhance their retention in breast cancer cells

To investigate mitochondrial targeting of the conjugated peptides, EMT6/AR-1 cells were incubated with fluorescein-labeled Str-H_8R_8 and VES-H_8R_8. Within 3 h of incubation in full medium, membrane association and cell penetration were evident. The fluorescence from both Str-H_8R_8 and VES-H_8R_8 indicate colocalization with the Mitotracker dye, which stains the mitochondria (Fig. S4A, B) [51]. Similarly to lipid-modified octaarginines, the cell uptake of both Str-H_8R_8 and VES-H_8R_8 are expected through the endolysosomal pathway [52]. The resultant bright and punctate signals, suggestive of endolysosomes, make it difficult to visualize peptide uptake into the mitochondria. Therefore, we quantified the peptide uptake in isolated mitochondria from peptide treated EMT6/AR-1 cells. Intact cells were incubated with either fluorescein-labeled Str-H_8R_8,VES-H_8R_8, H_8R_8, or free fluorescein for 3 h, and mitochondria were isolated through differential centrifugation [53]. The concentration of fluorescein in the isolated mitochondria was quantified and both Str-H_8R_8 and VES-H_8R_8 treated cells exhibited significantly higher uptake relative to H_8R_8 and free fluorescein ($p < .001$, Fig. 3A). Relative to Str-H_8R_8, VES-H_8R_8 treated cells exhibited significantly higher peptide uptake in the mitochondrial, possibly due to efflux inhibition on the plasma membrane and enhanced mitochondrial targeting ($p < .05$) [16]. Importantly, both Str-H_8R_8 and VES-H_8R_8 treated cells exhibited significantly higher peptide uptake in the mitochondria relative to H_8R_8, suggesting that the lipid modification of H_8R_8 is crucial for mitochondrial targeting ($p < .001$). Lipid-modified cationic peptides exhibit increased cell uptake due to enhanced membrane association and translocation, and hence increased mitochondrial uptake [41]. Therefore, we investigated the uptake of fluorescein-labeled Str-H_8R_8,VES-H_8R_8, H_8R_8, and free fluorescein in isolated mitochondria from untreated EMT6/AR-1 cells for 1 h. Isolated mitochondria treated with either Str-H_8R_8 or VES-H_8R_8 exhibited significantly higher peptide uptake relative to H_8R_8, confirming that lipid modification is required for mitochondrial uptake ($p < .001$, Fig. 3B). Interestingly, isolated mitochondria treated with VES-H_8R_8 exhibited significantly higher peptide uptake relative to Str-H_8R_8 ($p < .001$). VES is more hydrophobic than stearyl, which may be beneficial in penetrating the hydrophobic inner mitochondrial membrane [8]. Doxorubicin-resistant breast cancer cells have been shown to express efflux pumps on the mitochondrial membranes, such as breast cancer resistance protein (BCRP) and multi-drug resistance protein (MRP1) [54]. Relative to Str-H_8R_8, VES-H_8R_8 may also inhibit efflux pumps found on the mitochondrial membranes.

To investigate the role of VES-H_8R_8 on efflux pump inhibition [55], we compared the uptake and retention of fluorescein-labeled VES-H_8R_8 to that of Str-H_8R_8 with MDR breast cancer EMT6/AR-1 cells by flow cytometry. Interestingly, cell uptake was similar after 2 h of incubation; however, cells treated with VES-H_8R_8 showed significantly more fluorescein uptake at 5 and 24 h compared to those treated with Str-H_8R_8 ($p < .001$, Fig. 3C). To evaluate long-term retention of the peptides in the EMT6/AR-1 cells, the peptide-containing medium was removed after 24 h, and cells were left incubating for an additional 24 h in fresh medium. In these conditions, VES-H_8R_8 led to a ~8-fold higher retention in cells relative to that of Str-H_8R_8. Given that both amphiphiles should exhibit similar proteolytic stability, the increased uptake and retention observed for VES-H_8R_8 likely results from specific Pgp efflux inhibition. This observation is consistent with other studies where both vitamin E and VES have been shown to inhibit Pgp efflux in cancer cells [55]. Furthermore, PEGylated-VES is an established Pgp efflux inhibitor that has higher anti-cancer activity and greater efflux inhibition than VES alone [16]. Co-incubating VES and fluorescein-Str-H_8R_8 with EMT6/AR-1 cells led to a 12-fold increase in retention at 48 h vs. fluorescein-Str-H_8R_8 alone, further confirming the role of VES in Pgp efflux inhibition (Fig. S5). Thus, VES-H_8R_8 is an attractive amphiphile towards MDR treatment and would be more efficacious with the fluorescein replaced with a chemotherapeutic, such as doxorubicin, which would otherwise be effluxed by Pgp [56].

3.3. Lipid-modified cationic peptides affect mitochondria polarization and bioenergetics

We compared the effect of H_8R_8-based amphiphiles on mitochondria depolarization, using the JC-1 probe, to a series of controls, including the positive control of carbonyl cyanide *m*-chlorophenyl hydrazone (CCCP), which showed the lowest mitochondrial membrane potential (Fig. 4A). EMT6/AR-1 cells treated with H_8R_8-based amphiphiles showed significantly reduced mitochondrial membrane potential relative to all the controls (i.e., VES, stearic acid, unmodified peptide (H_8R_8), PEG-H_8R_8 and DMSO). Similar results were obtained with the parental cell line (Fig. S6A). These results suggest that mitochondria depolarization is involved in the cytotoxic mechanism of action of lipid-modified cationic peptides.

To better understand mitochondrial depolarization, we investigated VES-H_8R_8 and Str-H_8R_8 on the induction of mitochondrial permeability transition pore (mPTP). mPTP consists of adenine nucleotide translocase (ANT), cyclophilin D (CypD), and a voltage-dependent anion channel (VDAC), which together form a pore through the outer and inner mitochondrial membrane allowing for solutes < 1500 Da to leak out into the cytosol [57]. The presence of mitochondrial proteins in the cytoplasm induces intrinsic apoptosis [58]. We investigated the involvement of mPTP by inhibiting CypD binding with cyclosporine A (CsA), as previously reported [12]; however, since CsA is also a potent inhibitor of the Pgp efflux pump in the EMT6/AR-1 cells (and would result in JC-1 accumulation), we used EMT6/P cells to investigate the role of mPTP (Fig. 4B) [59]. While both Str-H_8R_8 and VES-H_8R_8 depolarized the mitochondria, in the presence of CsA, mitochondria polarization was maintained at levels similar to those of DMSO and CsA controls ($p > .05$), demonstrating the involvement of mPTP induction in the mechanism of action of H_8R_8-based amphiphiles. The CsA-

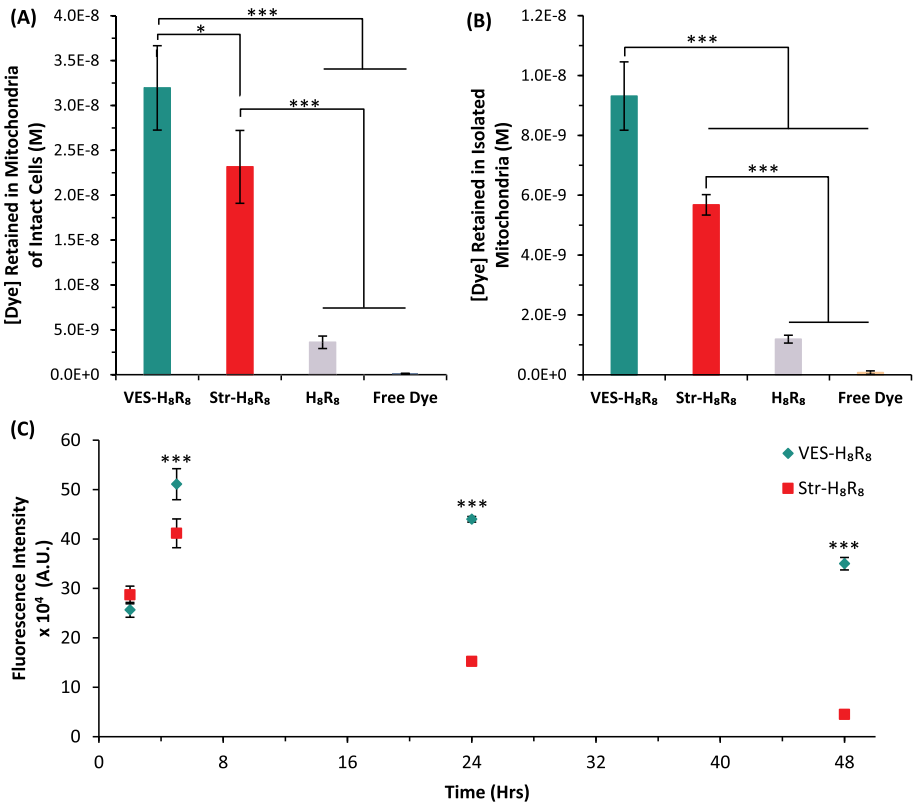

Fig. 3. Mitochondrial uptake and time-dependent uptake and retention of the H_8R_8-based amphiphiles. (A) Concentration of the dye retained in mitochondria isolated from EMT6/AR-1 cells upon a 3 h treatment of intact cells with either free dye, fluorescein, or fluorescein-labeled H_8R_8-based peptides. (B) Concentration of the dye retained in mitochondria isolated from EMT6/AR-1 cells upon a 1 h treatment of isolated mitochondria with either free dye or fluorescein-labeled H_8R_8-based peptides. Free dye was used as a negative control, whereas fluorescein modified H_8R_8 was used as a peptide control. (C) Time-dependent uptake and retention of fluorescein-labeled H_8R_8-based amphiphiles in EMT6/AR-1 cells during 2, 5 and 24 h incubation. Peptides were removed after 24 h, and the cells were incubated with fresh medium for another 24 h. Data are presented as a mean ± SD ($n = 3$) and statistical analysis performed using one-way ANOVA and Tukey's multiple comparison test (*$p < .05$, ***$p < .001$).

sensitive mitochondrial depolarization that we observed is consistent with that of guanidine-containing streptomycin and other cationic amphiphilic peptides, such as melittin and mastoparan [60,61]. Interestingly, decreased mitochondria membrane fluidity can induce mPTP, as may be the case with VES-H_8R_8 and Str-H_8R_8 treatment. This mechanism was observed with mastoparan, which interacts with the

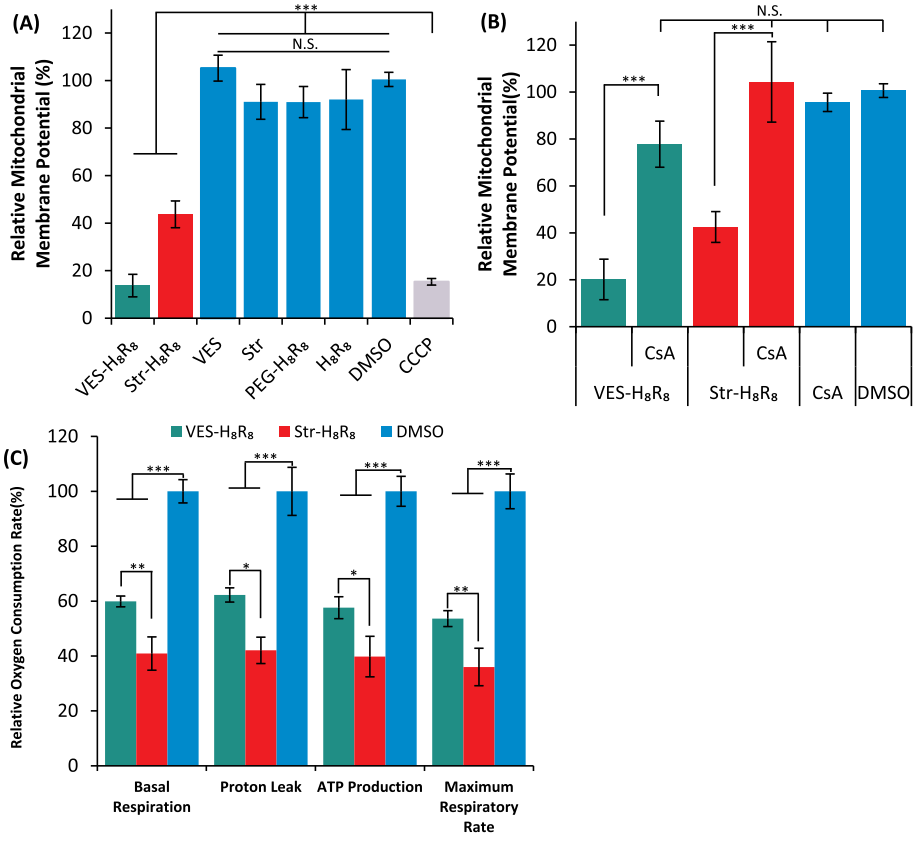

Fig. 4. H_8R_8-based amphiphiles depolarize mitochondria via a mitochondrial permeability transition pore (mPTP) dependent pathway and alter mitochondria bioenergetics. (A) The mitochondria membrane polarization of EMT6/AR-1 cells was measured after a 5 h treatment with Str-H_8R_8, VES-H_8R_8, or their controls, using the JC-1 probe and flow cytometry. (B) Using EMT6/P cells, mPTP-dependent depolarization was validated by co-incubating H_8R_8-based amphiphiles with cyclosporine A (CsA), an mPTP inhibitor, for 2 h. (C) Mitochondrial bioenergetic states of EMT6/AR-1 cells measured after incubation with H_8R_8-based amphiphiles for 2 h. Mitochondrial membrane potential and oxygen consumption rates are normalized to DMSO treated cells. Data are presented as mean ± SD ($n = 3$) and statistical analyses were performed using one-way ANOVA and Tukey's multiple comparison test (N.S. $p > .05$, *$p < .05$, **$p < .01$, ***$p < .001$).

lipid phase of the mitochondrial membrane [62,63]. VES alone can also induce mPTP, further supporting this mechanism for the VES-H_8R_8 treatment. Interestingly, with cationic polymers of higher molecular weight, such as PEI (> 25 kDa), CsA treatment did not maintain mitochondria polarization, possibly because PEI itself may form pores in the mitochondria membranes, allowing solutes to leak out [12,64].

Mitochondria bioenergetics were studied by measuring mitochondrial respiratory states in intact EMT6/AR-1 cells treated with H_8R_8-based amphiphiles using real-time measurements of oxygen consumption rates (OCR), as previously reported (Fig. 4C and Fig. S6B) [65]. Oligomycin was used to inhibit the mitochondrial F_0/F_1-ATP synthase, representing mitochondrial proton leak across the mitochondria inner membrane as a proxy for ATP production. Carbonylcyanide-*p*-trifluoromethoxyphenylhydrazone was used to measure the highest capacity of the electron transport chain, providing the maximum respiratory rate. All mitochondrial bioenergetics states of EMT6/AR-1 cells were significantly inhibited when treated with H_8R_8-based amphiphiles (Fig. 4C). Following a 2 h treatment, the basal respiration of EMT6/AR-1 cells were significantly inhibited compared to DMSO controls ($p < .001$). Furthermore, both cationic amphiphiles significantly inhibited proton leak, ATP production, and maximum respiratory rate relative to DMSO controls, which was expected as the proton current generated by basal respiration supports proton leak and ATP production ($p < .001$) [65]. Similar results were obtained in the parental cell line, EMT6/P (Fig. S6C). A decrease in ATP production directly affects Pgp-mediated drug efflux. For example, curcumin inhibited ATP production in doxorubicin resistant MCF7 cells, which led to efflux inhibition, and increased accumulation and retention of doxorubicin [30]. The changes in mitochondrial respiration states are consistent with other studies using cationic polymers where, for example, H1299 and C2C12 cells treated with linear or branched PEI had decreased basal respiration, proton leak, maximum respiration rate, and ATP production [22].

3.4. Lipid-modified cationic peptides induce ROS

mPTP induction and mitochondrial depolarization typically involve increased cellular levels of ROS, triggering complex signaling cascades that lead to cell death [1]. To test whether this was happening during the treatment of EMT6/AR-1 cells with H_8R_8-based amphiphiles, ROS levels were evaluated after treatment with Str-H_8R_8 and VES-H_8R_8, and compared to controls using 5-carboxy-2,7-dichlorodihydrofluorescein diacetate (CDCFDA) (Fig. 5). After 5 h of incubation with Str-H_8R_8 or VES-H_8R_8, ROS levels significantly increased to 200.9 ± 43.5% and 179.2 ± 26.3%, respectively ($p < .01$), which is similar to ROS levels with exposure to the positive control, hydrogen peroxide, of 266.7 ± 28.6%. Controls including VES, stearic acid, PEG-H_8R_8 and H_8R_8, did not increase ROS levels relative to DMSO controls ($p > .05$). Similar results were observed with the EMT6/P cells (Fig. S7A). Str-H_8R_8 significantly induced ROS after 2 h of incubation relative to controls whereas, surprisingly, VES-H_8R_8 did not ($p < .001$, Fig. S7B). Vitamin E has well-known antioxidant properties whereby the phenolic alcohol acts as a radical scavenger [66,67]. We therefore hypothesized that the delayed induction of ROS by VES-H_8R_8 was attributed to the cleavable ester present within vitamin E succinate, and subsequent radical scavenging. To test this hypothesis, we synthesized a vitamin *E*-modified H_8R_8 with a more stable butyl ether linker (VEB- H_8R_8) (Fig. S7C). Unexpectedly, however, treating EMT6/AR-1 cells for 2 h with the ether-linked VEB-H_8R_8 induced ROS levels comparable to those of the ester-linked VES-H_8R_8 (Fig. S7B). The ether linkage may be oxidized by intracellular reactive oxygen intermediates, cleaving vitamin E and thereby enabling ROS scavenging [68,69].

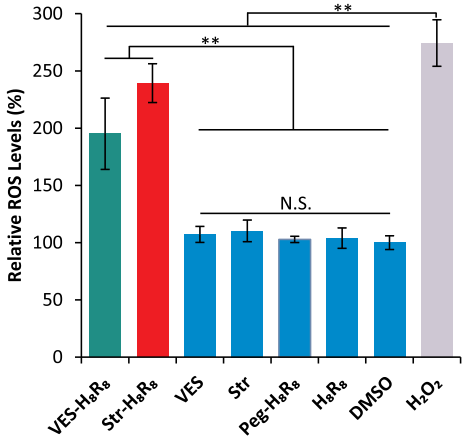

Fig. 5. Reactive oxygen species (ROS) levels are significantly increased upon treatment with H_8R_8-based amphiphiles. EMT6/AR-1 cells were incubated with treatment groups for 5 h followed by incubation with the CDFDA probe. Flow cytometry was used to determine relative ROS levels to DMSO controls. Data are presented as a mean ± SD ($n = 3$) and statistical analyses were performed using one-way ANOVA and Tukey's multiple comparison test (N.S. $p > .05$, $^{**}p < .01$).

3.5. Lipid-modified cationic peptides induce apoptosis, necrosis, and cell cycle arrest

Mitochondria depolarization and increased ROS levels often lead to apoptosis [65]; however, synthetic cationic polymers, such as PEI, have been reported to damage cell membranes and cause necrotic cell death [12,22]. To investigate the mechanism of cell death upon treatment with lipid-modified cationic peptides, annexin-V-Cy5 and 7-AAD were used to monitor the levels of apoptosis and necrosis, respectively [70]. Both Str-H_8R_8 and VES-H_8R_8 induced death of EMT6/AR-1 cells by apoptosis and necrosis significantly more than DMSO controls (Fig. 6A-C) and in a concentration-dependent manner (Fig. 6D-E). Consistent with their IC_{50} values, 5 μM of each of the lipid-modified cationic peptides had minimal effect compared to the DMSO control in terms of necrosis and apoptosis ($p > .05$). Interestingly, at 20 μM, VES-H_8R_8 treatment led predominately to apoptosis (46.9 ± 2.8%), which is similar to that observed with VES alone [71], whereas Str-H_8R_8 resulted in greater necrosis (44.2 ± 2.0%), which may be due to plasma membrane damage as was observed for other amphiphilic peptides [72,73].

H_8R_8-based amphiphile treatments were expected to arrest cells in a specific phase of the cell cycle as mitochondria depolarization and increased ROS levels should inhibit progression past cell cycle checkpoints [74]. We studied cell cycle distributions of EMT6/AR-1 cells treated with the H_8R_8-based amphiphiles by flow cytometry, using 7-AAD as a nucleic dye. Cells treated with Str-H_8R_8 and VES-H_8R_8 were arrested in the G1 cell cycle phase relative to DMSO controls (Figs. 6F and S8A–C, $p < .01$), which is consistent with the reported mechanisms of VES, pegylated-VES and melittin [71,75–77]. Consequently, there were fewer cells in the S (proliferation) and G2 cell cycle phases when treated with Str-H_8R_8 and VES-H_8R_8 vs. DMSO ($p < .001$). Similar results were observed in the EMT6/P cells (Fig. S8D). None of the controls, including VES, stearic acid, PEG-H_8R_8 and H_8R_8, significantly arrested the EMT6/P and EMT6/AR-1 cells in any phase (Fig. S8E, F). While it's not clear whether H_8R_8-based amphiphiles interact with any of the cell cycle regulatory or checkpoint proteins, sonic hedgehog signaling may be implicated based on its involvement with other cationic peptides [77].

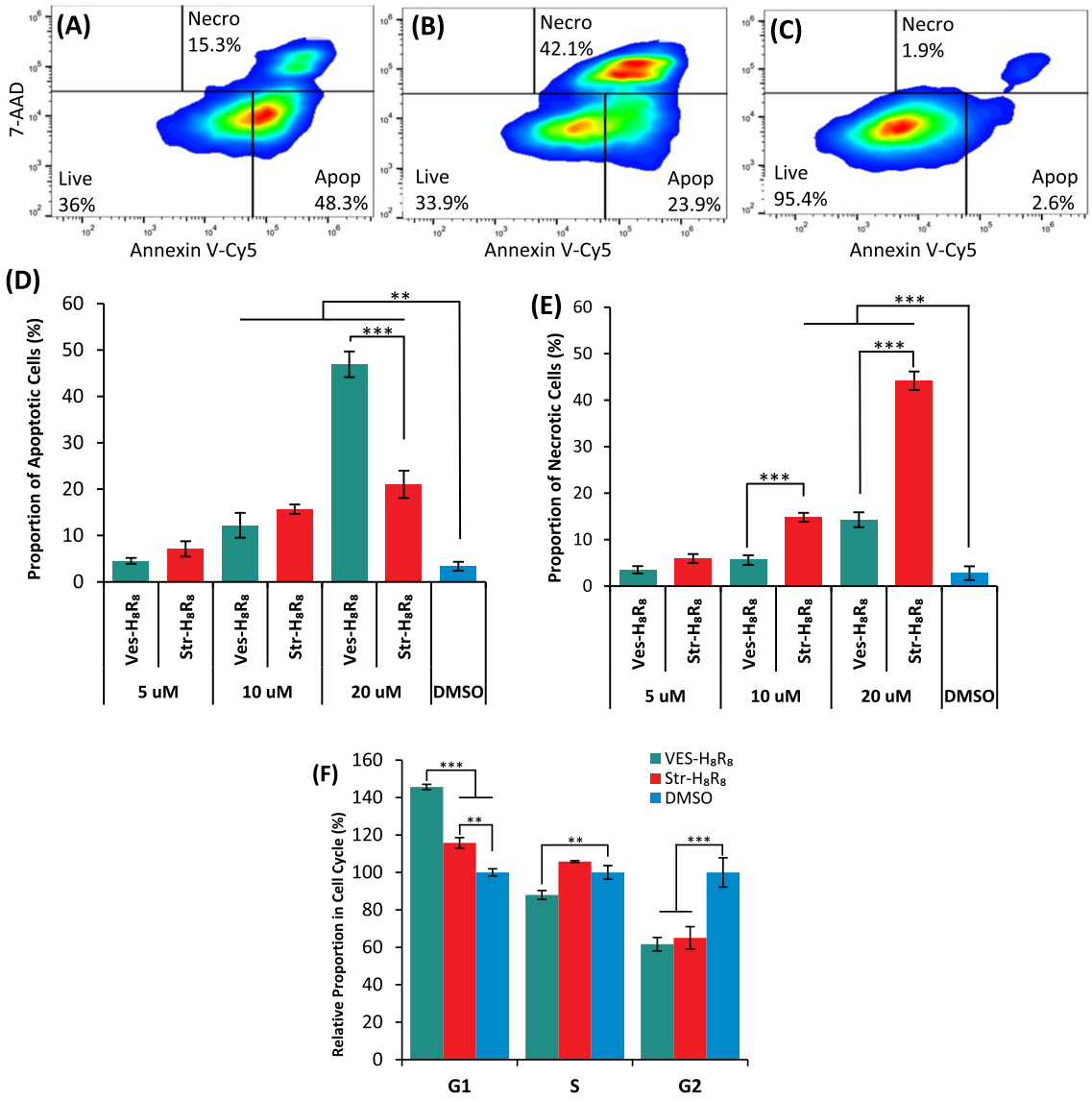

Fig. 6. Apoptosis, necrosis, and G_1 cell cycle arrest are induced upon treatment of EMT6/AR-1 with H_8R_8-based amphiphiles. Representative histograms of (A) VES-H_8R_8, (B) Str-H_8R_8, and (C) DMSO treated cells showing annexin-V-Cy5 (apoptosis) and 7-aminoactinomycin D (7-AAD) (necrosis) staining. Identical gates were set up to demonstrate the proportion of live, apoptotic (apop) and necrotic (necro) populations. (D) The proportion of cells in the apoptotic state upon treatment with either H_8R_8-based amphiphiles at 5, 10, and 20 μM or DMSO controls for 2 h. (E) The proportion of cells in a necrotic state upon treatment with either H_8R_8-based amphiphiles at 5, 10, and 20 μM or DMSO controls for 2 h. (F) The proportion of cells in G1, S or G2 phase when treated with the H_8R_8-based amphiphiles relative to that when treated with DMSO. Data are presented as a mean ± SD ($n = 3$) and statistical analyses were performed using one-way ANOVA and Tukey's multiple comparison test (N.S. $p > .05$, $^{**}p < .01$, $^{***}p < .001$).

4. Conclusions

Two lipid-modified cationic peptides, Str-H_8R_8 and VES-H_8R_8, were selectively cytotoxic to multi-drug resistant breast cancer cells in the low micromolar range, with VES-H_8R_8 showing greater selectivity and drug efflux inhibition. Similar to other cationic amphiphilic structures, lipid-modified cationic peptides target, disrupt and depolarize mitochondria, inhibit mitochondrial bioenergetics, decrease Pgp efflux, and induce ROS production. This leads to apoptosis and/or necrosis, and G1 cell cycle arrest. These properties of VES-H_8R_8 suggest its utility for chemotherapeutic delivery to MDR cancer cells in terms of enhanced uptake, retention, and anti-cancer activity.

Acknowledgments

We are grateful to the Shoichet Lab for thoughtful review and to the following for funding: Natural Sciences and Engineering Research Council of Canada (NSERC Discovery to MSS [RGPIN-2019-06933], NSERC CREATE M3 to PCC [CREAT 432258-13]) and Canadian Institutes of Health Research (CIHR Foundation to MSS [FDN-143276]).

Appendix A. Supplementary data

Supplementary data to this article can be found online at https://doi.org/10.1016/j.jconrel.2019.04.045.

References

[1] S. Weinberg, N. Chandel, Nat. Chem. Biol. 11 (1) (2015) 9–15.
[2] J. Dartier, E. Lemaitre, I. Chourpa, C. Goupille, S. Servais, S. Chevalier, K. Maheo, J.F. Dumas, Biochimica Et Biophysica Acta-General Subjects 1861 (5) (2017) 1075–1084.
[3] S. Kelley, Abstracts of Papers of the American Chemical Society, (2015), p. 249.
[4] P. Bugde, R. Biswas, F. Merien, J. Lu, D.-X. Liu, M. Chen, S. Zhou, Y. Li, Expert Opin.

Ther. Targets 21 (5) (2017) 511–530.
[5] K. Henkenius, B.H. Greene, C. Barckhausen, R. Hartmann, M. Marken, T. Kaiser, M. Rehberger, S.K. Metzelder, W.J. Parak, A. Neubauer, C. Brendel, E. Mack, Leuk. Res. 62 (2017) 56–63.
[6] K.V. Ledwitch, M.E. Gibbs, R.W. Barnes, A.G. Roberts, Biochem. Pharmacol. 118 (2016) 96–108.
[7] I.R. Indran, G. Tufo, S. Pervaiz, C. Brenner, Biochimica et Biophysica Acta (BBA)-Bioenergetics 1807 (6) (2011) 735–745.
[8] K. Horton, K. Stewart, S. Fonseca, Q. Guo, S. Kelley, Chem. Biol. 15 (4) (2008) 375–382.
[9] G. Bagkos, K. Koufopoulos, C. Piperi, Med. Hypotheses 83 (2) (2014) 175–181.
[10] S.R. Jean, D.V. Tulumello, C. Riganti, S.U. Liyanage, A.D. Schimmer, S.O. Kelley, ACS Chem. Biol. 10 (9) (2015) 2007–2015.
[11] M. Pereira, S. Kelley, J. Am. Chem. Soc. 133 (10) (2011) 3260–3263.
[12] G. Grandinetti, N. Ingle, T. Reineke, Mol. Pharm. 8 (5) (2011) 1709–1719.
[13] A. El-Sayed, I.A. Khalil, K. Kogure, S. Futaki, H. Harashima, J. Biol. Chem. 283 (34) (2008) 23450–23461.
[14] A. Ahmad, S. Ranjan, W.K. Zhang, J. Zou, I. Pyykko, P.K.J. Kinnunen, Biochimica Et Biophysica Acta-Biomembranes 1848 (2) (2015) 544–553.
[15] L. Prochazka, L.F. Dong, K. Valis, R. Freeman, S.J. Ralph, J. Turanek, J. Neuzil, Apoptosis 15 (7) (2010) 782–794.
[16] E.M. Collnot, C. Baldes, U.F. Schaefer, K.J. Edgar, M.F. Wempe, C.M. Lehr, Mol. Pharm. 7 (3) (2010) 642–651.
[17] X.-F. Wang, M. Birringer, L.-F. Dong, P. Veprek, P. Low, E. Swettenham, M. Stantic, L.-H. Yuan, R. Zobalova, K. Wu, Cancer Res. 67 (7) (2007) 3337–3344.
[18] A.S.A. Habeeb, Anal. Biochem. 14 (3) (1966) 328–336.
[19] K.E. Coan, B.K. Shoichet, J. Am. Chem. Soc. 130 (29) (2008) 9606–9612.
[20] C.P. Cerrato, M. Pirisinu, E.N. Vlachos, Ü. Langel, FASEB J. 29 (11) (2015) 4589–4599.
[21] A. Risso, E. Braidot, M.C. Sordano, A. Vianello, F. Macri, B. Skerlavaj, M. Zanetti, R. Gennaro, P. Bernardi, Mol. Cell. Biol. 22 (6) (2002) 1926–1935.
[22] A. Hall, L. Parhamifar, M.K. Lange, K.D. Meyle, M. Sanderhoff, H. Andersen, M. Roursgaard, A.K. Larsen, P.B. Jensen, C. Christensen, J. Bartek, S.M. Moghimi, BBA-Bioenergetics 1847 (3) (2015) 328–342.
[23] P. Sittisart, B. Chitsomboon, Evid. Based Complement. Alternat. Med. 2014 (2014) 1–11.
[24] S.V. Lale, A. Kumar, F. Naz, A.C. Bharti, V. Koul, Polym. Chem. 6 (11) (2015) 2115–2132.
[25] J. Ma, M. Shi, G. Li, N. Wang, J. Wei, T. Wang, J. Ma, Y. Wang, Int. J. Oncol. 43 (4) (2013) 1052–1058.
[26] Z. Duan, C. Chen, J. Qin, Q. Liu, Q. Wang, X. Xu, J. Wang, Drug Deliv. 24 (1) (2017) 752–764.
[27] A.I. Hashim, X. Zhang, J.W. Wojtkowiak, G.V. Martinez, R.J. Gillies, NMR Biomed. 24 (6) (2011) 582–591.
[28] D. Coman, Y. Huang, J.U. Rao, H.M. De Feyter, D.L. Rothman, C. Juchem, F. Hyder, NMR Biomed. 29 (3) (2016) 309–319.
[29] R.J. Gillies, N. Raghunand, G.S. Karczmar, Z.M. Bhujwalla, Journal of Magnetic Resonance Imaging 16 (4) (2002) 430–450.
[30] S. Guo, L. Lv, Y. Shen, Z. Hu, Q. He, X. Chen, Sci. Rep. 6 (2016) 21459.
[31] C.-P.H. Yang, C. Wang, I. Ojima, S.B. Horwitz, J. Nat. Prod. 81 (3) (2018) 600–606.
[32] M. Tomasetti, E. Strafella, S. Staffolani, L. Santarelli, J. Neuzil, R. Guerrieri, Br. J. Cancer 102 (8) (2010) 1224.
[33] T. Sakamoto, D.R. Hinton, H. Kimura, C. Spee, R. Gopalakrishna, S.J. Ryan, Graefes Arch. Clin. Exp. Ophthalmol. 234 (3) (1996) 186–192.
[34] K. Najjar, A. Erazo-Oliveras, D.J. Brock, T.-Y. Wang, J.-P. Pellois, J. Biol. Chem. 292 (3) (2017) 847–861.
[35] W.P. Verdurmen, P.H. Bovee-Geurts, P. Wadhwani, A.S. Ulrich, M. Hällbrink, T.H. van Kuppevelt, R. Brock, Chem. Biol. 18 (8) (2011) 1000–1010.
[36] C.G.A. Network, Nature 490 (7418) (2012) 61.
[37] J. Neuzil, T. Weber, N. Gellert, C. Weber, Br. J. Cancer 84 (1) (2001) 87.
[38] A. Roy, M. Murakami, M.J. Ernsting, B. Hoang, E. Undzys, S.-D. Li, Mol. Pharm. 11 (8) (2014) 2592–2599.
[39] X. Chen, T.K. Yeung, Z. Wang, Biochem. Biophys. Res. Commun. 277 (3) (2000) 757–763.
[40] J. Neuzil, Br. J. Cancer 89 (10) (2003) 1822.
[41] K.A. Lawson, K. Anderson, M. Simmons-Menchaca, J. Atkinson, L. Sun, B.G. Sanders, K. Kline, Exp. Biol. Med. 229 (9) (2004) 954–963.
[42] G. Bagkos, K. Koufopoulos, C. Piperi, Curr. Pharm. Des. 20 (28) (2014) 4570–4579.
[43] V.R. Fantin, J. St-Pierre, P. Leder, Cancer Cell 9 (6) (2006) 425–434.
[44] W.-H. Yoon, H.-D. Park, K. Lim, B.-D. Hwang, Biochem. Biophys. Res. Commun. 222 (3) (1996) 694–699.
[45] S. Ran, A. Downes, P.E. Thorpe, Proc. Am. Assoc. Cancer Res. 62 (2002) 6132–6140.
[46] W. Pham, M.F. Kircher, R. Weissleder, C.H. Tung, Chembiochem 5 (8) (2004) 1148–1151.
[47] D. Chu, W. Xu, R. Pan, P. Chen, RSC Adv. 5 (26) (2015) 20554–20556.
[48] D. Chu, W. Xu, R. Pan, Y. Ding, W. Sui, P. Chen, Nanomedicine 11 (2) (2015) 435–446.
[49] I.A. Khalil, Y. Hayashi, R. Mizuno, H. Harashima, J. Control. Release 156 (3) (2011) 374–380.
[50] Y. Hayashi, Y. Noguchi, H. Harashima, J. Control. Release 161 (3) (2012) 757–762.
[51] J. Adler, I. Parmryd, Cytometry Part A 77 (8) (2010) 733–742.
[52] S. Katayama, H. Hirose, K. Takayama, I. Nakase, S. Futaki, J. Control. Release 149 (1) (2011) 29–35.
[53] P. Azimzadeh, H.A. Aghdaei, P. Tarban, M.M. Akhondi, A. Shirazi, H.R.K. Khorshid, Gastroenterol. Hepatol. Bed to Bench 9 (2) (2016) 105.
[54] J. Dartier, E. Lemaitre, I. Chourpa, C. Goupille, S. Servais, S. Chevalier, K. Mahéo, J.-F. Dumas, Biochimica et Biophysica Acta (BBA)-General Subjects 1861 (5) (2017) 1075–1084.
[55] J.L. Tang, Q. Fu, Y.J. Wang, K. Racette, D. Wang, F. Liu, Cancer Lett. 336 (1) (2013) 149–157.
[56] X. Zeng, R. Morgenstern, A.M. Nyström, Biomaterials 35 (4) (2014) 1227–1239.
[57] J. Teixeira, R. Amorim, K. Santos, P. Soares, S. Datta, G.A. Cortopassi, T.L. Serafim, V.A. Sardão, J. Garrido, F. Borges, Toxicology 393 (2018) 123–139.
[58] K.W. Kinnally, P.M. Peixoto, S.-Y. Ryu, L.M. Dejean, Biochimica et Biophysica Acta (BBA)-Molecular Cell Res. 1813 (4) (2011) 616–622.
[59] M. Qadir, K.L. O'Loughlin, S.M. Fricke, N.A. Williamson, W.R. Greco, H. Minderman, M.R. Baer, Clin. Cancer Res. 11 (6) (2005) 2320–2326.
[60] M. Mather, H. Rottenberg, Biochimica et Biophysica Acta (BBA)-Bioenergetics 1503 (3) (2001) 357–368.
[61] D.R. Pfeiffer, T.I. Gudz, S.A. Novgorodov, W.L. Erdahl, J. Biol. Chem. 270 (9) (1995) 4923–4932.
[62] A. Colell, C. García-Ruiz, J.M. Lluis, O. Coll, M. Mari, J.C. Fernández-Checa, J. Biol. Chem. 278 (36) (2003) 33928–33935.
[63] T. Yamamoto, M. Ito, K. Kageyama, K. Kuwahara, K. Yamashita, Y. Takiguchi, S. Kitamura, H. Terada, Y. Shinohara, FEBS J. 281 (17) (2014) 3933–3944.
[64] V. Gogvadze, E. Norberg, S. Orrenius, B. Zhivotovsky, Int. J. Cancer 127 (8) (2010) 1823–1832.
[65] M. Brand, D. Nicholls, Biochem. J. 435 (2) (2011) 297–312.
[66] R. Yamauchi, Food Sci. Technol. Int. Tokyo 3 (4) (1997) 301–309.
[67] I. Nakanishi, T. Kawashima, K. Ohkubo, H. Kanazawa, K. Inami, M. Mochizuki, K. Fukuhara, H. Okuda, T. Ozawa, S. Itoh, Org. Biomol. Chem. 3 (4) (2005) 626–629.
[68] B. Reid, M. Gibson, A. Singh, J. Taube, C. Furlong, M. Murcia, J. Elisseeff, J. Tissue Eng. Regen. Med. 9 (3) (2015) 315–318.
[69] M. Browning, S. Cereceres, P. Luong, E. Cosgriff-Hernandez, J. Biomed. Mater. Res. A 102 (12) (2014) 4244–4251.
[70] S.L. Fink, B.T. Cookson, Infect. Immun. 73 (4) (2005) 1907–1916.
[71] K. Kanai, E. Kikuchi, S. Mikami, E. Suzuki, Y. Uchida, K. Kodaira, A. Miyajima, T. Ohigashi, J. Nakashima, M. Oya, Cancer Sci. 101 (1) (2010) 216–223.
[72] A. Lorents, P.K. Kodavali, N. Oskolkov, Ü. Langel, M. Hällbrink, M. Pooga, J. Biol. Chem. 287 (20) (2012) 16880–16889.
[73] S.M. Moghimi, P. Symonds, J.C. Murray, A.C. Hunter, G. Debska, A. Szewczyk, Mol. Ther. 11 (6) (2005) 990–995.
[74] E.S. Wenzel, A.T. Singh, In Vivo, vol. 32, (2018), pp. 1–5.
[75] C.M. Neophytou, C. Constantinou, P. Papageorgis, A.I. Constantinou, Biochem. Pharmacol. 89 (1) (2014) 31–42.
[76] H. Zhang, B. Zhao, C. Huang, X.-M. Meng, E.-B. Bian, J. Li, PLoS One 9 (5) (2014) e95520.
[77] X. Wu, B. Zhao, Y. Cheng, Y. Yang, C. Huang, X. Meng, B. Wu, L. Zhang, X. Lv, J. Li, Toxicol. Appl. Pharmacol. 288 (1) (2015) 74–83.